Available online at http://rgnaa.com
Commun. Nonlinear Anal. 1 (2022), 1–16
Research Article

Communications in Nonlinear Analysis
Publisher
Research Group of Nonlinear Analysis and Applications

Isolation Effect on Age-Stratified Compartmental Model of the COVID-19

Md. Shahidul Islam[a,*], K. M. Ariful Kabir[b], Jannatun Irana Ira[a], Mahadee Al Mobin[a], Md. Haider Ali Biswas[c], Praveen Kumar Gupta[d]

[a] *Department of Mathematics, University of Dhaka, Dhaka 1000, Bangladesh*
[b] *Department of Mathematics, Bangladesh University of Engineering and Technology, Dhaka, Bangladesh*
[c] *Mathematics Discipline, Khulna University, Khulna 9208, Bangladesh*
[d] *Department of Mathematics, National Institute of Technology, Silchar-788010, Assam, India*

Abstract

Focusing on the dynamics of the most recent outbreak of COVID-19, we formulate an age distributed model with five different components in terms of nonlinear partial differential equations. The model has been analyzed by studying the stability of the equilibrium points and their reproduction number. To explore the disease effect on different ages more efficiently, we apply the recent estimated data in the formulated model and analyze it numerically. From the model's numerical solution profiles, we observed more susceptibility and infection among the older population. Also studied the effectiveness of isolation in controlling illness and death.

Keywords: Age-structured, compartmental modeling, isolation effect, covid-19, SEIQR model.

1. Introduction

Epidemiology is the branch of science where infectious diseases are analyzed by modelling them mathematically. Modelling an epidemic helps us to study the behavior of the disease elaborately. It also helps us to understand the characteristics of the transmission of the disease and how it affects the population of a region and how severely it can affect the population. This population models can also be formulated focusing on a specific characteristic like age, gender etc. The age structured population model is constructed to study the behavior of the disease towards different aged individuals. Different diseases affect different aged population severely. It shows which part of the population is at high risk. For example, diseases like chicken pox and malaria highly affect the children whereas diseases like tuberculosis and AIDS affect the adults [21, 4].

*Corresponding author
Email addresses: mshahidul11@yahoo.com (Md. Shahidul Islam), k.ariful@yahoo.com (K. M. Ariful Kabir), zannatunirana@gmail.com (Jannatun Irana Ira), mamobin96@gmail.com (Mahadee Al Mobin), mhabiswas@yahoo.com (Md. Haider Ali Biswas), pkguptaitbhu@gmail.com (Praveen Kumar Gupta)

Received 2022-06-15

Coronavirus is an infectious disease which has spread globally and affected millions of life. It has been declared a pandemic by WHO after spreading in many countries since the first outbreak in China. It is a respiratory illness. The virus is transmitted through air or direct contact with patient. It attacks the respiratory system and may lead to pneumonia in severe cases. According to WHO situation report, 80% of the cases shows mild symptoms that gets recovered without any serious treatment. But rest of the 20% cases needs oxygen therapy as the virus damages the alveoli and makes it difficult to breathe. Also patients with chronic diseases like heart disease, diabetes, cancer etc faces critical situations.

To understand the disease characteristic we studied the SEIR model of COVID-19 in [17] with case study of Italy. Also we have studied COVID-19 epidemic models with different compartments like SEIQR model in [13] where the basic reproduction number and sensitivity analysis of the disease is discussed in details. We have seen some thorough discussion of Bangladesh case study with simple SIR model in [27]. SIR models with aged structure has been formulated and applied in case of various infectious diseases in [11]. Also for understanding the controlling strategies we studied the dynamical analysis of SEIRV model with quarantine and isolation policies in [2] and the SEIQR model with combination of quarantine and social distancing effect in [7]. The effect of the control on the economy has also been discussed in [15] using epidemiological models with behavioural dynamics from evolutionary game theory. A two-body exportation-importation model SEIQJR is formulated in [14] to demonstrate the consequences of border restrictions, medical resources, public counter compliancy etc. to control the spread of the disease. The dispersal effect to reduce the infection of COVID-19 in Bangladesh has been analyzed in [16]. The formulation of age structured model of cholera with vaccination and demographic movements are analyzed in [19]. We have also studied the age structured model with vertical transmission in [12].

The demography of COVID-19 based on age can be very useful for the pandemic event. By an age structured model we can identify which portion of the population is mostly affected by the virus. The data in [34] shows that 80 years or older population has nearly 15% fatality rate where children under 9 years old has 0% fatality rate. Therefore the older people are at more risk than other individuals. According to the recent data USA has 16% of older population that are 65 years or older and Italy has 22.8% [25]. These two countries are dealing with the most cases of deaths due to the virus. Since the pandemic is still ongoing, so it is still early to give any conclusion depending on this results. Therefore we take the help of mathematical modelling to understand the situation more elaborately.

Studying the age structured model can play a crucial role since the disease is affecting different aged population differently. The human body has an immune system that protects the body from any virus and fight with it by creating antibodies. Therefore, immune system can also fight against the coronavirus. But the virus is seen to damage our respiratory system if our immunity power is not strong enough. As a result, children and younger population with stronger immune system may not be affected by the virus as much as the elderly population or patients with lower immunity power. This less affected cases are identified as the mild cases. Due to weaker immune system the elders and individuals with chronic diseases are most likely to be at higher risk of getting infected easily and going into a critical condition. To Mathematically analyze this we formulate a model.

2. Age Structured Model Formulation

The age structured models of epidemics have specific groups of population depending on the disease. Most of the cases we have studied the age structured population model with 3 compartments and disease like AIDS, cholerae etc. can be modeled applying this model [21]. We studied the SIR, SIS age structured model formulations and its application in influenza disease transmission in [23] and the analysis of linear age-dependent population models and their optimal control in [3]. We have also studied the formulation of SEIR and MSEIR models for epidemics with continuous age structures along with their analysis and application in niger measles in [9, 22]. The application of SEIR model for chikunguniya with numerical simulations are discussed in [1]. Also an SEIRUS model is formulated to apply in age structured population of Nigeria to analyze disease control of AIDS [24].

Now by observing the characteristics of the coronavirus we consider 5 groups of individuals to model the age distribution. These are: $s(t,a), e(t,a), i(t,a), q(t,a)$ and $r(t,a)$. $s(t,a)$ is the susceptible population, $e(t,a)$ is the exposed population who are infected with the virus but asymptomatic, $i(t,a)$ is the infected population and they are symptomatic, $q(t,a)$ is the isolated population and $r(t,a)$ is the recovered population of age a at time t, where $a \in [0, a_\dagger)$ and $t \geq 0$ and $a_\dagger$ is the maximum age limit. The age structured COVID-19 model then can be written as,

$$\begin{cases} s_t(t,a) + s_a(t,a) = & -\big(\alpha(t,a) + \delta_1(a)\big)s(t,a) \\ e_t(t,a) + e_a(t,a) = & \alpha(t,a)s(t,a) - (\beta(a) + \delta_1(a))e(t,a) \\ i_t(t,a) + i_a(t,a) = & \beta(a)e(t,a) - \big(\mu(a) + \nu(a) + \delta_1(a) + \delta_2(a)\big)i(t,a) \\ q_t(t,a) + q_a(t,a) = & \nu(a)i(a,t) - \big(\gamma(a) + \delta_1(a) + \delta_2(a)\big)q(t,a) \\ r_t(t,a) + r_a(t,a) = & \mu(a)i(t,a) + \gamma(a)q(t,a) - \delta_1(a)r(t,a) \end{cases} \tag{2.1}$$

where the parameters,

- $\alpha(t,a)$ is the infection rate
- $\delta_1(a)$ is the natural death rate of age a population
- $\beta(a)$ is the rate at which the exposed individuals is transmitted to infected individuals
- $\mu(a)$ is the natural recovery rate for a aged population
- $\nu(a)$ is the rate of isolating the infected individuals and
- $\gamma(a)$ is the recovery rate of the isolated population.
- $\delta_2(a)$ is the disease induced death rate.

Now the model can be described by the following diagram:

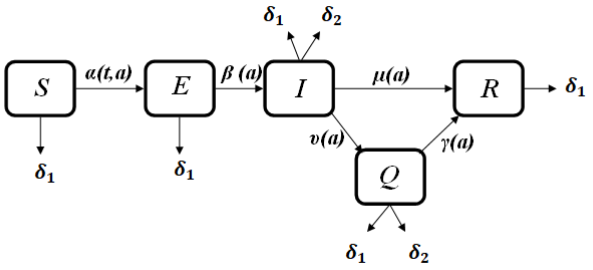

Figure 1: Diagram of the age structured model.

The model (2.1) is associated with the initial conditions,

$$\begin{cases} s(t,0) = \int_0^{a_\dagger} b(a)n(t,a)da,\ e(t,0) = i(t,0) = q(t,0) = r(t,0) = 0 \\ s(0,a) = s_0(a),\ e(0,a) = e_0(a),\ i(0,a) = i_0(a),\ q(0,a) = q_0(a),\ r(0,a) = r_0(a) \end{cases} \tag{2.2}$$

Here, we consider that all newly born population are susceptible and $b(a)$ is the birth rate, $s_0(a)$, $e_0(a)$, $i_0(a)$, $q_0(a)$ and $r_0(a)$ are the initial amount of susceptible, exposed, infected, quarantined and recovered population of age a.

Now we define the total susceptible population at time t, $S(t) = \int_0^{a_\dagger} s(t,a)da$. Similarly, $E(t) = \int_0^{a_\dagger} e(t,a)da$, $I(t) = \int_0^{a_\dagger} i(t,a)da$, $Q(t) = \int_0^{a_\dagger} q(t,a)da$ and $R(t) = \int_0^{a_\dagger} r(t,a)da$.

Let, $s(t,a) + e(t,a) + i(t,a) + q(t,a) + r(t,a) = n(t,a)$ be the age distributed population and the total population $N(t) = S(t) + E(t) + I(t) + Q(t) + R(t) = \int_0^{a_\dagger} n(t,a)da$.

The age-specific transmission rate of the susceptible individual is defined as,

$$\alpha(t,a) = \int_0^{a_\dagger} e(t,\omega) f(a,\omega) d\omega \tag{2.3}$$

where $e(t,\omega)$ is the exposed population and $f(a,\omega) = f_1^*(a) f_2(\omega)$ denotes the rate of transmission from exposed individual of age ω to susceptible individual of age a. hieme [30] suggested a specific form of $f_1^*(a)$ such that $f_1^*(a) = \kappa(a) f_1(a)$ is sufficiently concentrated in one particular age class, the endemic equilibrium can be destabilized even if it uniquely exists. So, we can concentrate where the solution is stable. Here $\kappa(a)$ is defined as in [20],

$$\kappa(a) = \frac{B}{b_0} a e^{-ka} y(t,a), \quad B > 0, a \geq 0 \quad \text{and } k > \delta_1^\infty = \operatorname{ess.sup}_{a \geq 0} \delta_1 \tag{2.4}$$

where $\kappa(a) \in (0, a_\dagger)$. Also let us define the probability of survival till age a [23],

$$\pi(a) = e^{-\int_0^a \delta_1(\tau)d\tau} \tag{2.5}$$

Now for the steady state of age distributed population as assumed in [22] , we let

$$\int_0^{a_\dagger} b(a) e^{-\int_0^a \delta_1(\tau)d\tau} da = 1 \tag{2.6}$$

from which we can write,

$$P^*(a) = n(0,a) = b_0 e^{-\int_0^a \delta_1(\tau)d\tau} \tag{2.7}$$

Now these conditions from (2.6) and (2.7) implies the following initial conditions for (2.1), $s_0(a) \geq 0, e_0(a) \geq 0, i_0(a) \geq 0, q_0(a) \geq 0, r_0(a) \geq 0$ and $P^*(a) = n(0,a) = s_0(a) + e_0(a) + i_0(a) + q_0(a) + r_0(a)$. Using this in (2.7) we have,

$$b_0(a) = \frac{s_0(a) + e_0(a) + i_0(a) + q_0(a) + r_0(a)}{e^{-\int_0^{a_\dagger} \delta_1(\tau)d\tau}}$$

2.1. Normalization

To normalize the model in (2.1) we let,

$$x(t,a) = \frac{s(t,a)}{P^*(a)}, y(t,a) = \frac{e(t,a)}{P^*(a)}, z(t,a) = \frac{i(t,a)}{P^*(a)}, u(t,a) = \frac{q(t,a)}{P^*(a)}, v(t,a) = \frac{r(t,a)}{P^*(a)}$$

And the age-specific transmission rate, $\alpha^*(t,a) = \int_0^{a_\dagger} \kappa(a) y(t,a) P^*(a) da$, where we defined $\kappa(a)$ previously in (2.4). So, $\alpha^*(t,a)$ becomes,

$$\alpha^*(t,a) = B \int_0^{a_\dagger} a e^{-ka} y(t,a) da \tag{2.8}$$

This specific function for transmission rate is concentrated in one specific age class and will be used in analyzing the stability of endemic equilibrium later in this paper.
So (2.1) becomes,

$$\begin{cases} x_t(t,a) + x_a(t,a) = & -\alpha^*(t,a)x(t,a) \\ y_t(t,a) + y_a(t,a) = & \alpha^*(t,a)x(t,a) - \beta(a)y(t,a) \\ z_t(t,a) + z_a(t,a) = & \beta(a)y(t,a) - \big(\mu(a) + \nu(a)\big)z(t,a) \\ u_t(t,a) + u_a(t,a) = & \nu(a)z(a,t) - \gamma(a)u(t,a) \\ v_t(t,a) + v_a(t,a) = & \mu(a)z(t,a) + \gamma(a)u(t,a) \end{cases} \tag{2.9}$$

with the initial conditions,

$$x(t,0)=1,\ y(t,0)=z(t,0)=u(t,0)=v(t,0)=0$$
$$x(0,a)=x_0(a), y(0,a)=y_0(a), z(0,a)=z_0(a), u(0,a)=u_0(a), v(0,a)=v_0(a)$$

3. Basic Reproduction Number and Stability Analysis

3.1. Basic Reproduction Number

To determine the basic reproduction number of the system (2.1) we follow the method described in [23] for SIR model. At first since the system at equilibria is time independent so, it is converted into an age specific SIR model. From this age specific system the disease free equilibrium (DFE) is obtained by setting $i(a)=0, r(a)=0$ and infection force $\hat{\lambda}=0$. Then to find endemic equilibria the infection force $\hat{\lambda}$ is set non-zero. While finding the endemic equilibrium, it is obtained that $s(a)$ is an arbitrary constant and the infective $i(a)$ gives an implicit expression containing $\hat{\lambda}$. Finally, replacing $i(a)$ in the definition of $\hat{\lambda}$ the basic reproduction number of the SIR model is generated. Now following this method for system (2.1) we generate the expression of R_0 here.

First we determine the equilibriums to formulate the reproduction number. The equilibria are time-independent solutions of the system (2.1). Here we consider the maximum age, $a_\dagger=\infty$ Therefore, we can write the model as,

$$\begin{cases} s_a(a) = & -\big(\alpha(a)+\delta_1(a)\big)s(a) \\ e_a(a) = & \alpha(a)s(a)-(\beta(a)+\delta_1(a))e(a) \\ i_a(a) = & \beta(a)e(a)-\big(\mu(a)+\nu(a)+\delta_1(a)\big)i(a) \\ q_a(a) = & \nu(a)i(a)-\big(\gamma(a)+\delta_1(a)\big)q(a) \\ r_a(a) = & \mu(a)i(a)+\nu(a)q(a)-\delta_1(a)r(a) \end{cases} \tag{3.1}$$

and the associated conditions are,

$$s(0)=\int_0^\infty b(a)n(a)da,\ e(0)=i(0)=q(0)=r(0)=0$$

Then for time independent age-specific transmission rate we define, $\alpha(a)=\hat{\alpha}f_1(a)$ where,

$$\hat{\alpha}=\int_0^\infty f_2(\omega)e(\omega)d\omega$$

Now for the disease free equilibrium (DFE) let, $e=i=q=r=\hat{\alpha}=0$ and so we get,

$$s(a)=s(0)\pi(a)$$

Then for the endemic equilibrium, let $\hat{\alpha}\neq 0$, then

$$s(a)=s(0)e^{-\int_0^a(\hat{\alpha}f_1(s)+\delta_1(s))ds}$$

To determine the value of $s(0)$, adding all the equations of (3.1),

$$n_a=-\delta_1(a)n(a)$$

Solving which we obtain,

$$n(a)=n(0)\pi(a)$$

where we can define, $n(0)=\frac{\int_0^{a_\dagger}n_0(a)da}{\pi(a)}=\phi_0$. So we get,

$$s(0)=\phi_0\int_0^\infty b(a)\pi(a)da=\phi_0$$

Since from (2.6) we have, $\int_0^\infty b(a)\pi(a)da = 1$. Therefore, $s(0)$ is also a constant and we can write,

$$s(a) = \phi_0 e^{-\int_0^a (\hat{\alpha} f_1(s)+\delta_1(s))ds} \tag{3.2}$$

Now solving the equation of exposed population using the integrating factor $e^{\int_0^a (\delta_1(\sigma)+\beta(\sigma))d\sigma}$ and the boundary condition $e(0) = 0$.

$$e(a) = \hat{\alpha} \int_0^a f_1(\eta)s(\eta)e^{-\int_\eta^a [\delta_1(\sigma)+\beta(\sigma)]d\sigma} d\eta \tag{3.3}$$

From equation (3.2) we have, $s(\eta) = \phi_0 e^{-\int_0^\eta \hat{\alpha} f_1(s)ds} e^{-\int_0^\eta \delta_1(s)ds} = \phi_0 \pi(a) e^{-\int_0^\eta \hat{\alpha} f_1(s)ds}$, using which in (3.3) we get,

$$e(a) = \phi_0 \hat{\alpha} \pi(a) \int_0^a f_1(\eta) e^{-\int_0^\eta \hat{\alpha} f_1(s)ds} e^{-\int_\eta^a [\delta_1(\sigma)+\beta(\sigma)]d\sigma} d\eta$$

Since, $e(a)$ is not explicit in the equation, so we replace $e(a)$ from $\hat{\alpha} = \int_0^\infty f_2(\omega)e(\omega)d\omega$. Hence we find,

$$\begin{aligned}
\hat{\alpha} &= \phi_0 \hat{\alpha} \int_0^\infty f_2(a)\pi(a) \left[\int_0^a f_1(\eta) e^{-\int_0^\eta \hat{\alpha} f_1(s)ds} e^{-\int_\eta^a \beta(\sigma)d\sigma} d\eta \right] da \\
\Rightarrow 1 &= \phi_0 \int_0^\infty f_2(a)\pi(a) \left[\int_0^a f_1(\eta) e^{-\int_0^\eta \hat{\alpha} f_1(s)ds} e^{-\int_\eta^a \beta(\sigma)d\sigma} d\eta \right] da
\end{aligned}$$

Let

$$G(\hat{\alpha}) = \phi_0 \int_0^\infty f_2(a)\pi(a) \left[\int_0^a f_1(\eta) e^{-\int_0^\eta \hat{\alpha} f_1(s)ds} e^{-\int_\eta^a \beta(\sigma)d\sigma} d\eta \right] da$$

In our consideration, $f_(a) > 0$ which implies that, $G(\hat{\alpha})$ is a strictly decreasing function. So, if $G(\hat{\alpha}) = 1$ has a positive solution then it is unique [23]. Also, $\lim_{\hat{\alpha}\to\infty} G(\hat{\alpha}) = 0$. So, the existence of a positive solution of $G(\hat{\alpha}) = 1$ depends on $G(0)$.

Therefore, we define the reproduction number:

$$R_0 = \phi_0 \int_0^\infty f_2(a)\pi(a) \left[\int_0^a f_1(\eta) e^{-\int_\eta^a \beta(\sigma)d\sigma} d\eta \right] da \tag{3.4}$$

Hence, it is clear from the above equations that, $G(\hat{\alpha}) = 1$ has a unique positive solution when $R_0 > 1$. So, for $R_0 > 1$ the model described in (2.1) has a unique Endemic equilibrium.

3.2. Stability Analysis of the Disease Free Equilibrium

From the previous section we have observed that the system (2.1) has a disease free equilibrium which is, $(s^0(a), e^0(a), i^0(a), q^0(a), r^0(a)) = (s(a) = s(0)\pi(a), 0, 0, 0, 0)$.

Now to analyze the stability, we linearize the equations of (2.1) for perturbation, as done in [23, 22] and let

$$\begin{aligned}
s(a,t) &= \bar{s}(a,t) + s^0(a), \\
e(a,t) &= \bar{e}(a,t) + e^0(a), \\
i(a,t) &= \bar{i}(a,t) + i^0(a), \\
q(a,t) &= \bar{q}(a,t) + q^0(a), \\
r(a,t) &= \bar{r}(a,t) + r^0(a)
\end{aligned}$$

where $(\bar{s}, \bar{e}, \bar{i}, \bar{q}, \bar{r})$ be the perturbations in DFE. Then the system (2.1) becomes,

$$\begin{cases}
\bar{s}_t(t,a) + \bar{s}_a(t,a) = -\alpha(t,a)s^0(a) \\
\bar{e}_t(t,a) + \bar{e}_a(t,a) = \alpha(t,a)s^0(a) - \beta(a)\bar{e}(t,a) \\
\bar{i}_t(t,a) + \bar{i}_a(t,a) = \beta(a)\bar{e}(t,a) - \big(\mu(a) + \nu(a)\big)\bar{i}(t,a) \\
\bar{q}_t(t,a) + \bar{q}_a(t,a) = \nu(a)\bar{i}(a,t) - \gamma(a)\bar{q}(t,a) \\
\bar{r}_t(t,a) + \bar{r}_a(t,a) = \mu(a)\bar{i}(t,a) + \gamma(a)\bar{q}(t,a)
\end{cases} \tag{3.5}$$

where,

$$\alpha(t,a) = \hat{\alpha} f_1(a)$$
$$\bar{s}(t,0) = \int_0^\infty b(a)\bar{n}(a)da, \bar{e}(t,0) = \bar{i}(t,0) = \bar{q}(t,0) = \bar{r}(t,0) = 0$$

Let the solution of (3.5) are,

$$\bar{s}(t,a) = \bar{s}(a)e^{\lambda t}$$
$$\bar{e}(t,a)) = \bar{e}(a)e^{\lambda t}$$
$$\bar{i}(t,a) = \bar{i}(a)e^{\lambda t}$$
$$\bar{q}(t,a) = \bar{q}(a)e^{\lambda t}$$
$$\bar{r}(t,a) = \bar{r}(a)e^{\lambda t}$$

Then we get the following system using these equations where we use a dependent functions instead of a and t dependent functions since its more convenient [23].

$$\begin{cases} \bar{s}_a(a) = -\lambda\bar{s}(a) - \bar{\alpha} \\ \bar{e}_a(a) = -\lambda\bar{e}(a) + \bar{\alpha} - \beta(a)\bar{e}(t,a) \\ \bar{i}_a(a) = -\lambda\bar{i}(a) + \beta(a)\bar{e}(t,a) - \big(\mu(a) + \nu(a)\big)\bar{i}(t,a) \\ \bar{q}_a(a) = -\lambda\bar{q}(a) + \nu(a)\bar{i}(a,t) - \gamma(a)\bar{q}(t,a) \\ \bar{r}_a(a) = -\lambda\bar{r}(a) + \mu(a)\bar{i}(t,a) + \gamma(a)\bar{q}(t,a) \end{cases} \tag{3.6}$$

where,

$$\bar{\alpha} = \bar{\hat{\alpha}} f_1(a)$$
$$\bar{s}(t,0) = \int_0^\infty b(a)\bar{n}(a)da, \bar{e}(t,0) = \bar{i}(t,0) = \bar{q}(t,0) = \bar{r}(t,0) = 0$$

Now by applying the previous method, we solve the first two equation of (3.6), we get

$$H(\lambda) = \phi_0 \int_0^\infty f_2(a)\pi(a)\left[\int_0^a f_1(\eta)e^{-\int_\eta^a(\beta(s)+\lambda)ds}d\eta\right]da$$

From where we can have, $H(0) = R_0$.

We observe that, $H'(\lambda) < 0$, $H(\lambda)$ is a decreasing function when $\lambda > 0$ and increasing function when $\lambda < 0$. Also the equation in RHS of $H(\lambda)$ has a unique negative real solution if and only if $H(0) = R_0 < 1$ and a unique positive real solution of $R_0 > 1$ or $R_0 = 1$. Then from [23, 22] we can see that, every complex solution $\lambda = \epsilon_1 \pm i\epsilon_2$, we have $|H(\lambda)| < 1$ which means that the DFE is locally asymptotically stable if $R_0 < 1$ and if $R_0 > 1$ the DFE is unstable.

3.3. Stability Analysis of the Endemic Equilibrium

To analyze the behavior of the endemic equilibrium point we take first two equations from the normalized equations in (2.9),

$$\begin{cases} x_t(t,a) + x_a(t,a) = -\alpha^*(t,a)x(t,a) \\ y_t(t,a) + y_a(t,a) = \alpha^*(t,a)x(t,a) - \beta(a)y(t,a) \end{cases} \tag{3.7}$$

where $t > 0, a > 0$ and the initial conditions are,

$$\begin{cases} x(t,0) = 1,\ y(t,0) = 0,\ x(0,a) = x_0(a),\ y(0,a) = y_0(a) \\ \alpha^*(t,a) = B\int_0^{a_\dagger} ae^{-ka}y(t,a)da,\ t > 0,\ a \geq 0. \end{cases} \tag{3.8}$$

Since the rest of the equation does not affect the dynamics of the equation (3.7) so we can only remove them to analyze the stability. To reduce the system of PDEs in a four-dimensional system of ODEs we apply the method described in [20] and let

$$\begin{cases} X(t) = & \int_0^{a_\dagger} e^{-ka}x(t,a)da \\ Y(t) = & \int_0^{a_\dagger} e^{-ka}y(t,a)da \\ L(t) = & B\int_0^{a_\dagger} ae^{-ka}x(t,a)da \\ \Lambda(t) = & B\int_0^{a_\dagger} ae^{-ka}y(t,a)da \end{cases} \tag{3.9}$$

Differentiating the equations in (3.9) we get the following ODEs:

$$\begin{cases} \frac{dX(t)}{dt} = 1 - [k + \Lambda(t)]X(t) \\ \frac{dY(t)}{dt} = X(t)\Lambda(t) - (k+\beta)Y(t) \\ \frac{dL(t)}{dt} = BX(t) - [k + \Lambda(t)]L(t) \\ \frac{d\Lambda(t)}{dt} = BY(t) + L(t)\Lambda(t) - (k+\beta)\Lambda(t) \end{cases} \tag{3.10}$$

with the initial conditions, $X(0) = X_0,\ Y(0) = Y_0,\ L(0) = L_0,\ \Lambda(0) = \Lambda_0$, where $t > 0$ and $(X_0, Y_0, L_0, \Lambda_0) \in \mathbb{R}^4_+$. Then the endemic equilibrium $E_1 = (X^*, Y^*, L^*, \Lambda^*)$ can be derived easily by solving the following system of equations:

$$\begin{aligned} &1 - [k + \Lambda^*(t)]X^*(t) = 0 \\ &X^*(t)\Lambda^*(t) - (k+\beta)Y^*(t) = 0 \\ &BX^*(t) - [k + \Lambda^*(t)]L^*(t) = 0 \\ &BY^*(t) + L^*(t)\Lambda^*(t) - (k+\beta)\Lambda^*(t) = 0 \end{aligned}$$

We get the following equations from the above system,

$$\begin{cases} X^* = \frac{1}{k+\Lambda^*} \\ Y^* = \frac{\Lambda^*}{(k+\beta)(k+\Lambda^*)} \\ L^* = \frac{B}{(k+\Lambda^*)^2} \\ \Lambda^* = \frac{\Lambda^*}{(k+\beta)}\left[\frac{B}{(k+\beta)(k+\Lambda^*)} + \frac{B}{(k+\Lambda^*)^2}\right] \end{cases} \tag{3.11}$$

Then from the last equation of (3.11) we get,

$$F(\Lambda^*) = \frac{B}{(k+\beta)}\left[\frac{1}{(k+\beta)(k+\Lambda^*)} + \frac{1}{(k+\Lambda^*)^2}\right] = 1 \tag{3.12}$$

where $F(\Lambda^*)$ is clearly a decreasing function for $\Lambda^* > 0$ and therefore we can have reproduction number R_0 by letting $R_0 = F(0)$, so

$$R_0 = \frac{B(2k+\beta)}{k^2(k+\beta)^2} \tag{3.13}$$

Now the equation (3.12) has a unique positive root Λ^*, by which we can say that, there exists a unique endemic equilibrium point E_1.

Next to analyze the stability of the equilibrium we write the Jacobian matrix of the system (3.10) at E_1 as follows:

$$J = \begin{pmatrix} -(k+\Lambda^*) & 0 & 0 & -X^* \\ \Lambda^* & -(k+\beta) & 0 & X^* \\ B & 0 & -(k+\Lambda^*) & -L^* \\ 0 & B & \Lambda^* & L^* - (k+\beta) \end{pmatrix}$$

Then by equating the characteristic polynomial of the matrix it is shown in [20] that the endemic equilibrium E_1 is asymptotically stable if and only if $a_1a_2a_3 > a_0a_3^2 + a_1^2$ where,

$$\begin{aligned} a_0 &= \frac{B}{X^*}(1 - kX^*) + 2(k+\beta)B(1 - kX^*) \\ a_1 &= \frac{2B}{(k+\beta)X^*} + 3B(1 - kX^*) + B + (k+\beta)BX^*(1 - kX^*) \\ a_2 &= \frac{1}{X^{*2}} + \frac{4B}{k+\beta} + 2BX^* + (1 - kX^*)BX^* \\ a_3 &= \frac{2}{X^*} + \frac{2BX^*}{k+\beta} + BX^{*2} \end{aligned}$$

and these a_0, a_1, a_2 and a_3 are the coefficients of the eigenvalue λ in the characteristic polynomial.

4. Numerical Results and Discussions

To solve the system numerically we estimate the parameter values first. Considering the normalized system described in (2.9), the parameter values are estimated from the collected data [28, 26, 29, 6]. Since the recent data of Bangladesh was not available so data of Belgium (till 31st December,2020) is collected here.

Table 1: Parameter values.

β		γ	
Age	Normalized	Age	Normalized
0-9	0.03213	0-9	0.071
10-19	0.1454	10-19	0.0681
20-29	0.2268	20-29	0.0656
30-39	0.1987	30-39	0.063
40-49	0.1969	40-49	0.0618
50-59	0.176	50-59	0.0592
60-69	0.1204	60-69	0.0567
70-79	0.1219	70-79	0.0544
80+	0.2801	80+	0.0497

μ		ν	
Age	Normalized	Age	Normalized
0-9	0.069	0-9	0
10-19	0.068	10-19	0.012
20-29	0.065	20-29	0.02
30-39	0.062	30-39	0.02
40-49	0.06	40-49	0.07
50-59	0.059	50-59	0.10
60-69	0.056	60-69	0.171
70-79	0.054	70-79	0.207
80+	0.051	80+	0.06

For $\alpha^*(t,a)$ value in equation (2.8) we assumed $R_0 = 2.5$, $k = 0.25$ and $y = \frac{365}{15days} = 24\ years$ from which we determine the value of B as shown in [20],

$$B = \frac{k^2(k+y)^2}{2k+y}R_0 = 3.7504$$

We also assumed the death rate, $\delta_2 = 0.26e^{0.01a}$ for the calculations. The initial populations used in the calculation are given in the following tables [33].

Table 2: Initial population.

Initial Susceptible Population		**Initial Exposed Population**		**Initial Infected Population**	
Age	Normalized	Age	Normalized	Age	Normalized
0-9	0.9998	0-9	2.29×10^{-4}	0-9	2.07×10^{-4}
10-19	0.9997	10-19	3.67×10^{-4}	10-19	3.34×10^{-4}
20-29	0.997	20-29	3.34×10^{-3}	20-29	3.01×10^{-3}
30-39	0.9966	30-39	3.87×10^{-3}	30-39	3.37×10^{-3}
40-49	0.9958	40-49	4.89×10^{-3}	40-49	4.18×10^{-3}
50-59	0.9954	50-59	5.45×10^{-3}	50-59	4.62×10^{-3}
60-69	0.8438	60-69	4.18×10^{-3}	60-69	3.66×10^{-3}
70-79	0.9937	70-79	7.14×10^{-3}	70-79	6.27×10^{-3}
80+	0.9764	80+	2.83×10^{-2}	80+	2.36×10^{-2}

Initial Isolated Population	
Age	Normalized
0-9	0
10-19	3.9×10^{-6}
20-29	6.04×10^{-5}
30-39	6.7×10^{-5}
40-49	2.92×10^{-4}
50-59	4.62×10^{-4}
60-69	6.27×10^{-4}
70-79	1.3×10^{-3}
80+	9.43×10^{-3}

Initial Recovered Population	
Age	Normalized
0-9	1.36×10^{-4}
10-19	2.18×10^{-4}
20-29	1.96×10^{-3}
30-39	2.16×10^{-3}
40-49	2.64×10^{-3}
50-59	2.77×10^{-3}
60-69	2.16×10^{-3}
70-79	3.72×10^{-3}
80+	1.26×10^{-2}

Using these parameter values and initial data we have formulated the solution graphs using finite difference method [18] to analyze them in details. The graphs of susceptible, exposed, infected, quarantined and recovered population over age and time for different age groups 15-20, 25-30, 35-40, 45-50, 55-60, 65-70, 75-80, 85-90 are discussed here.

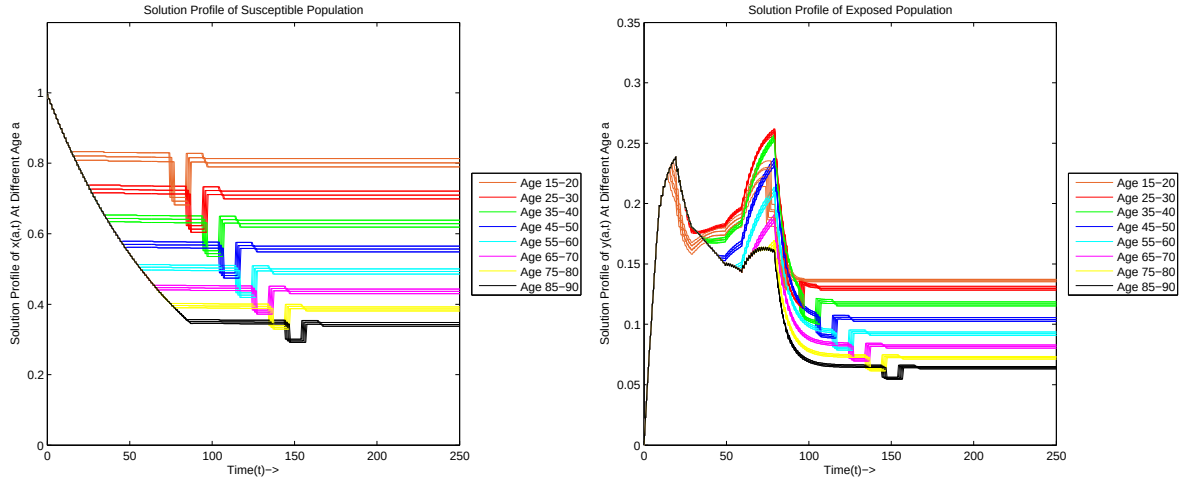

From Figure 2, we observe the followings:

- In the first graph, as we go from top to bottom of an age group the value at which the susceptible population becomes stable over time decreases. From the graph we can see that the susceptible population density decreases fast for higher age group in comparison to a lower age group which indicates low susceptibility among young population and high susceptibility among the adults.
- By observing the density of exposed population, the value at which the exposed population shows

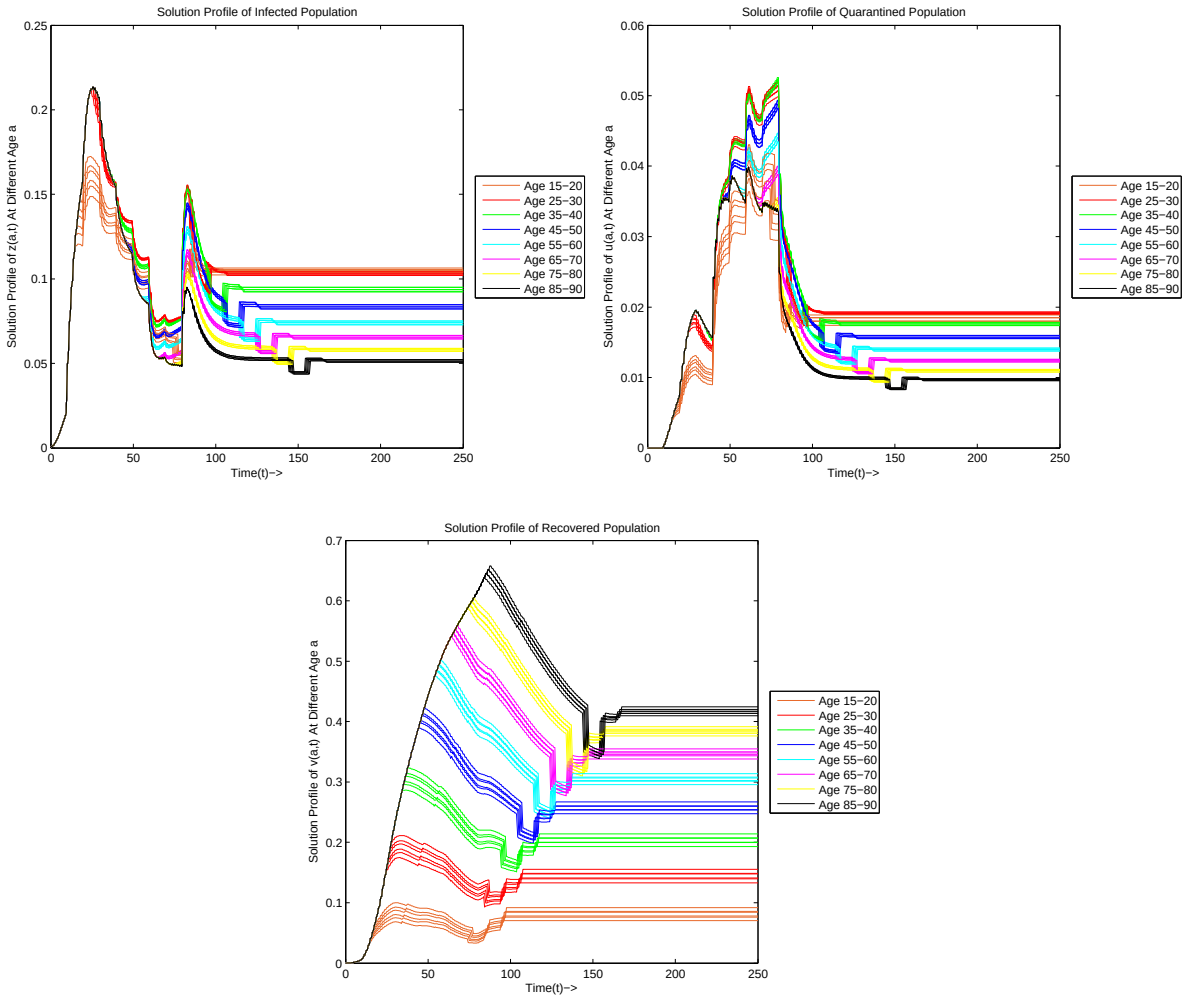

Figure 2: The solution profile of densities of $x(t,a), y(t,a), z(t,a), u(t,a)$ and $v(t,a)$ for different age groups encoded by different colors.

fluctuation decreases over time. We see that elder people get more exposed at the beginning and over time the population decreases since they start getting infected at a higher rate.

- The solution profile of infected population over time shows that initially, the quantity of population with more age is higher than the younger age and the opposite scenario is observed over the time. Due to high fatality rate and hospitalization rate of higher age population the older population quickly decreases in numbers here.

- The solution graphs of isolated population clearly shows that the isolated population density decrease fast for higher age group in comparison to a lower age group due to higher removal rate among higher age group. It shows that the older population has lower immunity power and low survival chances.

- We can also observe that the solution profile of $z(t,a)$ initially after reaching to a peak value it drops down drastically as the isolation rate increases that exact time and the graph of $u(t,a)$ reaches its peak. Then infected population increases again as isolation drops down. Therefore when isolation rate is high, infection drops down and when isolation rate is low the infection spreads more.

- From the last graph we observe that, as we go from top to bottom of an age group the value at which the recovered population shows fluctuation over time increases. It also shows that the older population has the higher recovery profile. But in reality this is not true. In the 1st graph we see that the young

population has the least susceptibility of being infected. So, a very small amount of population flows through the compartments and so the quantity remains low in recovered population. Since a large number of older population is infected over time, therefore we see a large older population in the last compartment.

4.1. Effect of Controlled Isolation on Infection and Death

Now we turn our attention to the best preventive strategies to minimize the infection by applying non-pharmaceutical control interventions in absence of effective vaccine. Introducing several optimal control strategies have great impact to prevent the older people from being infected and thus to combat the spread of the pandemic COVID-19. One such time variant control policy in the form of home-quarantine has been shown effective in [8]. Moreover, the impact of developing self-immunity, specially for the aged people by taking physical exercise and immune boosting foods has been shown promising to reduce the infection [5]. To show the effectiveness of control measures, we consider the isolation as parametric control strategy in reducing the disease burden. Contagious diseases are known to be less infectious if we can implement better isolation measure. Same is also seen in this case. Here in our age structured model with partial differential equations (PDEs), the isolation rate is considered to be $\nu(a)$.
Let us introduce a control parameter p which represents the strictness of the isolation effort. Thus we redefine the isolation rate as

$$\nu^*(a) = p \times \nu(a),$$

where the allowed value of p is in the range $[0, 5]$ to respect the trivial conditions imposed on rates of the model. Now taking different values of the control parameter p from the interval $[0, 5]$, we solve our model numerically and the results obtained from this simulation is presented in Figure 3.

The set of images in Figure 3 exhibits the decrease of infected population with the increase of control parameter, p. The first graph shows us the dynamics of infected population without any isolation (since isolation rate is assumed zero). Then sequentially increasing the rate we observe the reduction of the peak value of the infected population. It has been found in calculations from the above graph that the infected population without any isolation shown in Figure 3 can be **decreased up to 16.55% in peak values and 30.73% in stable values**.

Similarly, the isolation effect on disease induced death has been calculated. The set of images of Figure 4 exhibits the decrease of death of infected population with the increase of control parameter, p. Calculating from the peak values of the graph, the infected population's death without any isolation shown in Figure can be **decreased up to 16.59% in peak values and 32.05% in stable values**.

5. Conclusions

Age-stratified mathematical model with age specific transmission of five compartments for COVID-19 has been structured and analyzed in this paper. Then the basic reproduction number R_0 has been determined of the model and then we observed that when $R_0 < 1$, the DFE is asymptotically stable and when $R_0 > 1$, the DFE is unstable. Similarly, the endemic equilibrium's stability is also analyzed. After that, the model is solved numerically and also examined with the real world data. We used the age distributed data of Belgium. From obtained solution graphs we noticed that the older population are more susceptible and get infected by the virus more significantly. We also observe the relation between the infection and isolation from these graphs and how they change with each other. When the isolation rate gets higher the number of infected population drops down and when isolation process slows down the infection spreads and number of patient rises. To analyze this effect more thoroughly, we then study the number of infected population

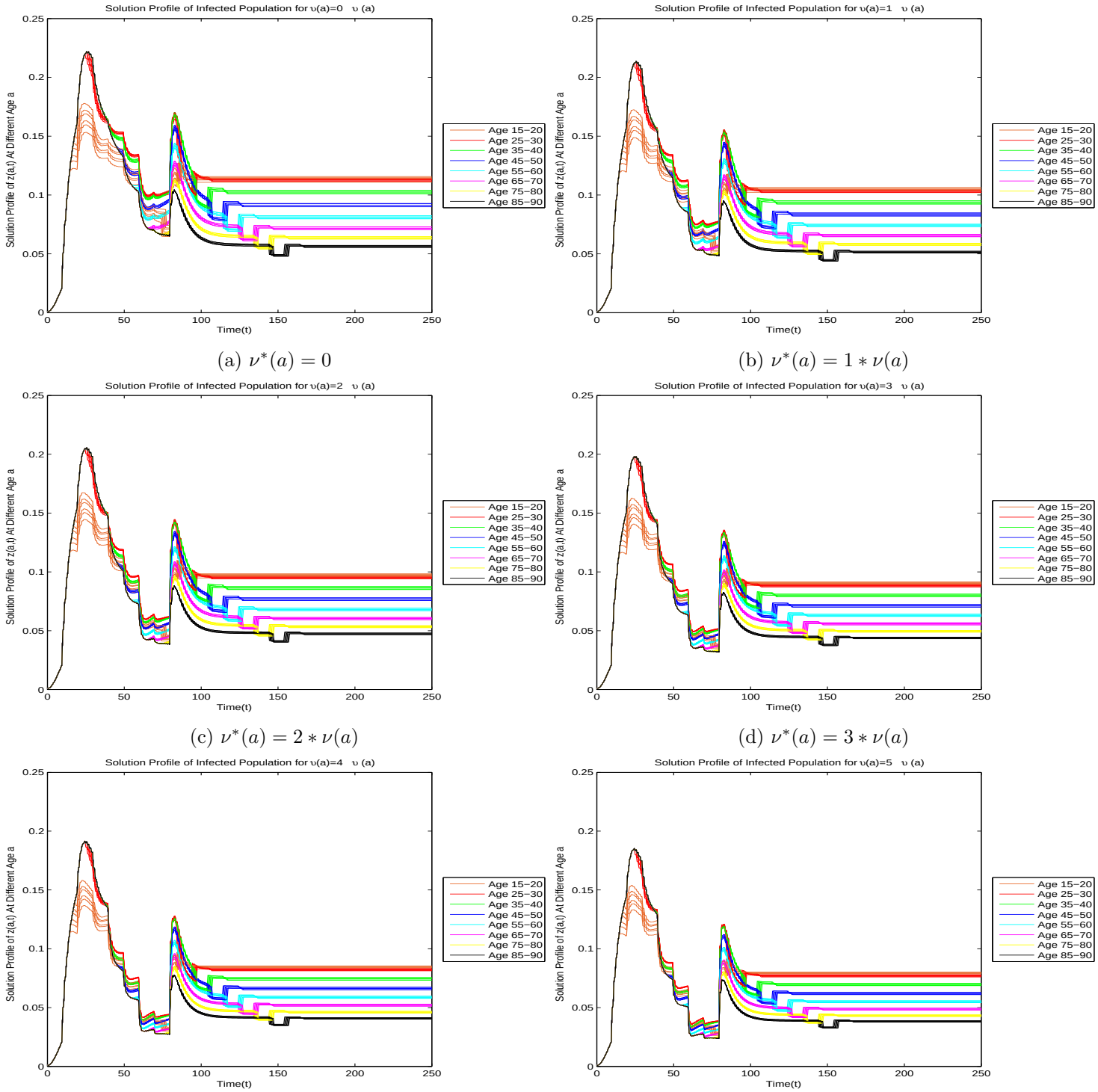

(a) $\nu^*(a) = 0$

(b) $\nu^*(a) = 1 * \nu(a)$

(c) $\nu^*(a) = 2 * \nu(a)$

(d) $\nu^*(a) = 3 * \nu(a)$

(e) $\nu^*(a) = 4 * \nu(a)$

(f) $\nu^*(a) = 5 * \nu(a)$

Figure 3: Effect of controlled isolation on infected population

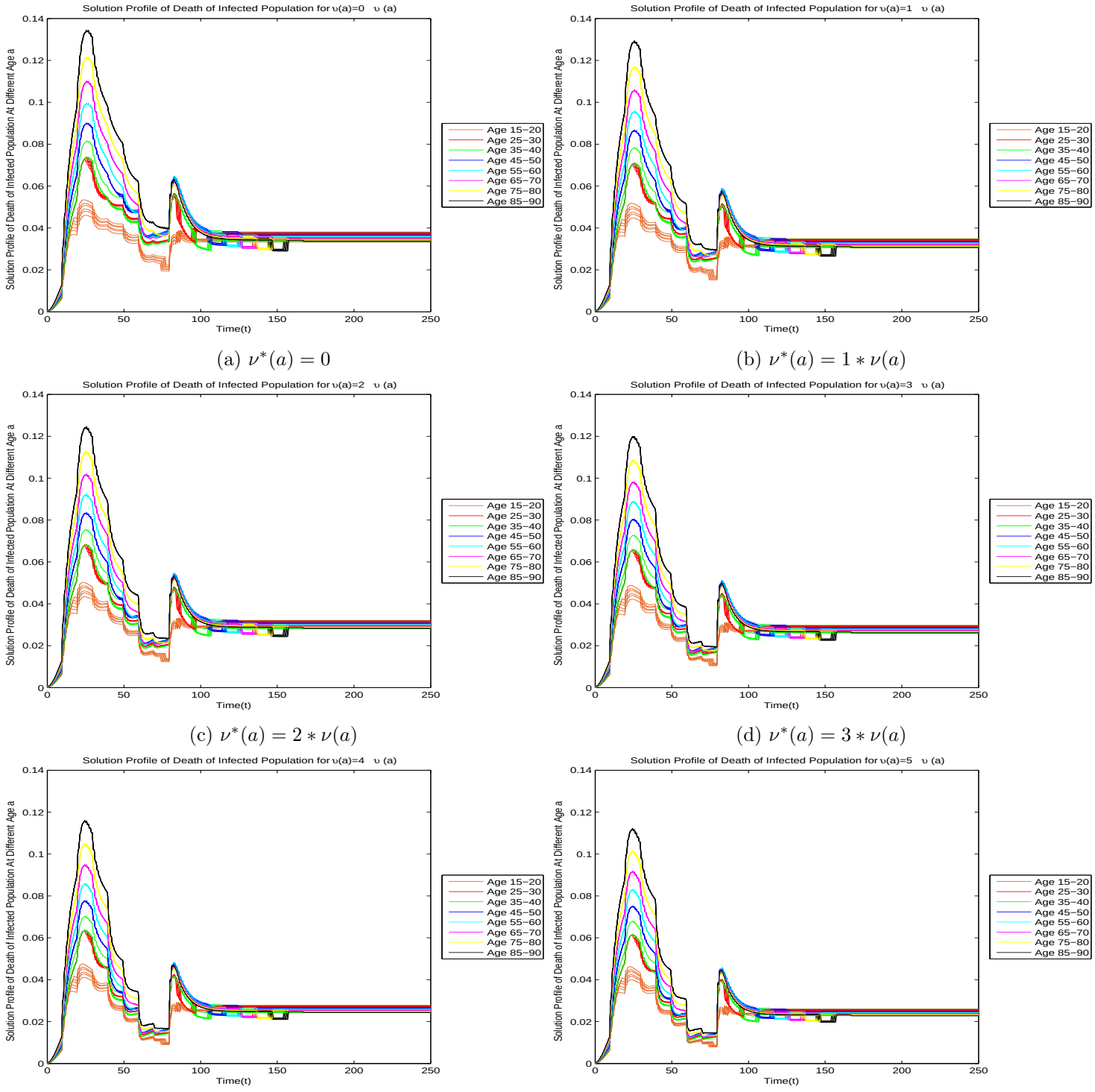

(a) $\nu^*(a) = 0$ (b) $\nu^*(a) = 1 * \nu(a)$

(c) $\nu^*(a) = 2 * \nu(a)$ (d) $\nu^*(a) = 3 * \nu(a)$

(e) $\nu^*(a) = 4 * \nu(a)$ (f) $\nu^*(a) = 5 * \nu(a)$

Figure 4: Effect of controlled isolation on disease induced death of infected population

and deaths for different scenarios by changing the isolation control parameter. For that analysis, we used the Belgium data and we calculated that by increasing the isolation parameter five time it's current value, the peak value of the infected population can be reduced up to 16.55% and the peak of the death numbers can be dropped down by 16.59%. So, our findings suggest that the age-structured model can be effectively applied to measure the COVID-19 situation at different ages demographically and can also be used to make important decisions on controlling this global pandemic by adopting proposed control strategies based on the disease dynamics.

References

[1] F.B. Agusto , S. Easley, K. Freeman, M. Thomas, *Mathematical model of three age-structured transmission dynamics of Chikungunya virus*, Comput. Math. Methods M., (2016). 2

[2] M. Alam, K.M.A. Kabir, J. Tanimoto, *Based on mathematical epidemiology and evolutionary game theory, which is more effective: quarantine or isolation policy?*, J. Stat. Mech. 033502. (doi:10.1088/1742-5468/ab75ea) (2020). 1

[3] S. Anita, *Analysis and Control of Age-Dependent Population Dynamics*, Springer Science & Business Media, (2000). 2

[4] M.H.A. Biswas, M.M. Haque, U.K. Mallick, *Optimal Control Strategy for the Immunotherapeutic Treatment of HIV Infection with State Constraint*, Optim. Control Appl. Methods, **40(4)** (2019), 807–818. 1

[5] M.H.A. Biswas, A.I. Islam, S. Akter, S. Mondal, M.S. Khatun,S.A. Samad, A.K. Paul, M.R. Khatun, *Modelling the Effect of Self-Immunity and the Impacts of Asymptomatic and Symptomatic Individuals on COVID-19 Outbreak*, Comput. Model Eng. Sci., **125(3)** (2020), 1033–1060. 4.1

[6] https://www.brusselstimes.com/ 4

[7] A. Chowdhury, K.M.A. Kabir, J. Tanimoto, *How quarantine and social-distancing policy can suppress the outbreak of novel coronavirus in developing or under poverty level countries: a mathematical and statistical analysis.*, (2020). (doi: 10. 21203/rs.3.rs-20294/v1) 1

[8] J.A.M. Gondim, L. Machado, *Optimal quarantine strategies for the COVID-19 pandemic in a population with a discrete age structure*, Chaos Solitons Fractals, **140** (2020), 110–166. 4.1

[9] H.W. Hethcote, *Age-Structured Epidemiology Models and Expressions For R_0, Mathematical Understanding Of Infectious Disease Dynamics*, World Sci. Publ., (2009) 91–128. 2

[10] F. Hoppensteadt, *An age dependent epidemic model*, J. Franklin Inst., **297(5)** (1974), 325–333.

[11] M. Iannelli, *The Mathematical Modelling of Epidemics*, UNITEXT - La Matematica per il 3 piu 2. **79** (2005). 1

[12] H. Inaba, *Mathematical Analysis of an Age-Structured SIR Epidemic Model with Vertical Transmission*, Discrete. Contin. Dyn. Syst. Ser. A., **6** (2006), 69–96. 1

[13] M.S. Islam, J. Irana Ira, K.M.A. Kabir, M. Kamrujjaman, *Effect of Lockdown and Isolation to Suppress the COVID-19 in Bangladesh: An Epidemic Compartments Model*, J. Appl. Math. Comput., **4(3)** (2020), 83–93. 1

[14] K.M.A. Kabir, A. Chowdhury, J. Tanimoto, *Impact of border enforcement measures, medical resources, and public counter compliancy on the global spread of the novel COVID-19: two-body export-importation epidemic*, Preprints (2020), 2020050242. (doi:10. 20944/preprints202005.0242.v1) 1

[15] K.M.A. Kabir, J. Tanimoto, *Evolutionary game theory modelling to represent the behavioural dynamics of economic shutdowns and shield immunity in the COVID-19 pandemic* R. Soc. Open Sci., **7**(2020). (http://dx.doi.org/10.1098/rsos.201095) 1

[16] M.H. Kabir, M.O. Gani, S. Mandal, M.H.A. Biswas, *Modeling the dispersal effect to reduce the infection of COVID-19 in Bangladesh*, Sensors., **1** (2020), 100043. 1

[17] M. Kamrujjaman, U. Ghosh, M.S. Islam, *Pandemic and the Dynamics of SEIR Model: Case COVID-19*, Preprints, (2020). 1

[18] A. Khan, G. Zaman, *Global analysis of an age-structured SEIR endemic model*, Chaos Solitons Fractals, **108** (2018), 154–165. 2

[19] E. Kokomo, Y. Emvudu, *Mathematical analysis and numerical simulation of an age-structured model of cholera with vaccination and demographic movements*, Nonlinear Anal. Real World Appl., **45** (2019), 142-156. 1

[20] T. Kuniya, *Stability Analysis of an Age-Structured SIR Epidemic Model with a Reduction Method to ODEs*, Math., **6(9)** (2018), 147. 2, 3.3, 3.3, 1

[21] J. Li, F. Brauer, *Continuous-Time Age-Structured Models in Population Dynamics and Epidemiology, Mathematical Epidemiology*, Springer, Berlin, **1945** (2008), 205–227. 1, 2

[22] X.Z. Li, B. Fang, *Stability of An Age-Structured SEIR Epidemic Model with Infectivity in Latent Period*, Appl. Appl. Math. **4** (2009), 218–236. 2, 2, 3.2, 3.2

[23] M. Martcheva, *An Introduction to Mathematical Epidemiology*, New York, Springer, (2015). 2, 2, 3.1, 3.1, 3.2, 3.2, 3.2

[24] V.A. Okhuese,e O.H. Kehind, *Application of an age-structured deterministic endemic model for disease control in Nigeria*, Eng. Math. Lett., (2020). 2

[25] https://www.prb.org/countries-with-the-oldest-populations/ 1
[26] https://public.opendatasoft.com/explore/dataset/covid-19-pandemic-belgium-deaths-agesexdate/table/?disjunctive.region&disjunctive.agegroup&disjunctive.sex&sort=date 4
[27] M.H.B. Siam, M.M. Hasan, E. Raheem, M.H.R. Khan, M.H. Siddiqee, M.S. Hossain, *Insights into the first wave of the COVID-19 pandemic in Bangladesh: Lessons learned from a high-risk country*, medRxiv,(2020). 1
[28] https://www.statista.com/statistics/1114426/confirmed-coronavirus-cases-in-belgium-by-age/ 4
[29] https://www.statista.com/statistics/523463/population-of-belgium-by-age-group/ 4
[30] H. Thieme, *Stability change of the endemic equilibrium in age-structured models for the spread of S-I-R type infectious diseases, Differential Equations Models in Biology, Epidemiology and Ecology*, Springer, Berlin, **92** (1991), 139-158. 2
[31] H. Wendland, *Error Estimates for Interpolation by Compactly Supported Radial Basis Functions of Minimal Degree*, J. Approx. Theory, **93** (1998), 258–272.
[32] H. Wendland, *Piecewise polynomial, positive definite and compactly supported radial functions of minimal degree*, Adv. Comput. Math., **4** (1995), 389–396.
[33] https://en.wikipedia.org/wiki/COVID-19_pandemic_in_Belgium 1
[34] https://www.worldometers.info/coronavirus/coronavirus-age-sex-demographics/